https://doi.org/10.20965/jaciii.2015.p0185

Paper:

A Switched Extend Kalman-Filter for Visual Servoing Applied in Nonholonomic Robot with the FOV Constraint

Yuan Fang, Zhang Xiaoyong, Huang Zhiwu, Wentao Yu, and Yabo Wang

School of Information Science and Engineering, Central South University
Changsha, Hunan 410075, China
E-mail: zxyong@gmail.com

[Received July 1, 2014; accepted November 13, 2014]

In this paper, a switched Kalmanfilter (KF) is used to predict the status of feature points leaving the field of view (FOV), which is one of the most common constraints in FOV. By using the prediction of status to compensate for the real state of feature points, nonholonomic robots conduct visual servoing tasks efficiently. Results of simulation and experiments verify the effectiveness of the proposed approach.

Keywords: EKF, FOV, visual servoing, control, nonholonomic robot

1. Introduction

Visual servoing is a robot control strategy that uses visual feedback to drive a robot moving from its initial position to a desired one. Visual servoing involves many constraints. One of the most common being the field of view (FOV). The FOV constraint, i.e., keeping feature points in the field of view, is a basic requirement for capturing feature points used to achieve visual feedback control [1]. Traditionally, the studies on visual servoing have been concentrated in the six-degree-of-freedom robot manipulators [2–4], in which FOV constraints have been studied by many experts, Mezouar and Chaumette [5], for example, proposed a potential method for generating a path in image space and then using an IBVS algorithm to enable a six-degree-of-freedom (6 DOF) manipulator to track the generated path on the image plane. In [6] Chesi and Hung exploited a path planning approach for robot manipulators that took the FOV constraint into account by minimizing a cost function.

In contrast, we subjected a mobile robot to nonholonomic constraints, which brings greater challenges to our servoing task [7]. This problem of the mobile robot has been addressed by experts. For example, in [8] López-Nicolás and Bhattacharya proposed a switched servoing controller to construct an optimal servoing trajectory for the robot under the FOV constraint, this contoller combines a straight line and a T-curve. One disadvantage of this approach is that T-curve is usually oversensitive to visual measurement disturbance. In [9] Fang et al fixed an active camera on the mobile robot, then developed an adaptive camera tracking controller to keep feature points within the FOV of camera. However this technique requires that the camera spin 360° a function is not available for all nonholonomic robots. Robustness and efficiency issues also limit the applications of these methods.

Many methods relies on temporal-filtering (TF), specifically, a Kalman-filter (KF) to address robustness and efficiency issues. A 3-D pose and its time rate constitute a 12-D state vector to be estimated in real time, meaning that many of these filtering methods, such as particle filters [10], can not model true distribution well in real time. A true 3-D pose estimation using Kalman filter (KF) for RVS has been realized in [11]. With KF, photogrammetric equations are formed by first mapping object features in the camera frame, then projecting them onto the image plane. KF is then applied to provide an implicit, recursive solution of pose parameters. The filter output model for RVS is nonlinear in system states, so an extended KF (EKF) is usually applied, in which case output equations are linearized for the current state estimates. The use of a KF in RVS is motivated by its several advantages, including its recursive implementation, capability of statistically combining redundant information (such as features) or sensors, temporal filtering, possibility of using lower number of feature points, and the possibility for changing the measurement set without disrupting operation [11, 12]. An EKF-based platform [13] was proposed, for instance, to integrate a range sensor with a vision sensor for estimating robust poses in RVS. Additionally, EKF implementation also facilitates dynamic windowing of features of interest by estimating the next time-step feature location. This enables only small window areas to be processed in image-parameter measurement and significantly reduces image-processing time. It has been shown that, in practice, an EKF provides near-optimal estimation [11]. Despite its advantages, its main constraint, the FOV constraint, remains to be solved.

Inspired by the above studies, we propose a visual servoing approach for helping solve the FOV problem. i.e., a switched EKF (SEKF). The SEKF both enhances servoing control robustness and improves the efficiency of the servoing process while satisfying FOV constraints. Results of simulation and experiments prove that even though some feature points leave the camera FOV, it remains highly possible for the robot to accomplish visual

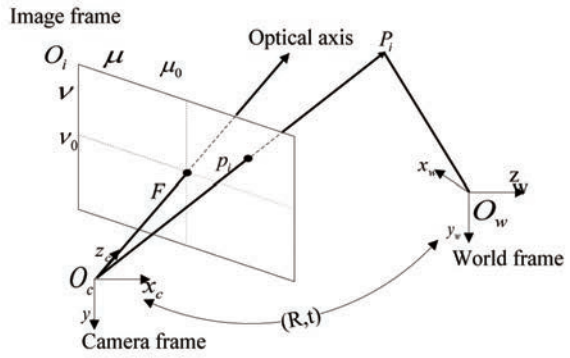

Fig. 1. Perspective camera model.

servoing tasks by using the EKF prediction function.

The remainder of this paper is organized as follows: In Section 2, we analyze camera models in our system. In Section 3, we detail the improved EKF. In Section 4 we demonstrate how simulation and experiment results show the effectiveness of our approach.

2. Model Analysis

2.1. Camera Model

The perspective camera model in **Fig. 1** is commonly used, as detailed in [14, 15].

As shown in **Fig. 1**, O_c is considered to be the optical center of the pinhole camera. Coordinates $\{O_c, x_c, y_c, z_c\}$ are the camera frame. Coordinates $\{O_i, \mu, \nu\}$ are the image frame, and p_i on the plane are the projections of feature point p_i. The relationship between P_i $\{O_c, x_c, y_c, z_c\}$ and $p_i\{O_i, \mu, \nu\}$ is described as follows:

$$p_i = K\,[R|t]\,P_i \quad \ldots\ldots\ldots\ldots\ldots\ldots \quad (1)$$

Where R, t are rotation and translation between world coordinates and camera coordinates generally called extrinsic camera parameters. K is the camera parameter matrix of intrinsic parameter, which is defined as follow:

$$K = \begin{bmatrix} Fk_u & Fk_u\cot\varphi & \mu_0 \\ 0 & \dfrac{Fk_v}{\sin\varphi} & \nu_0 \\ 0 & 0 & 1 \end{bmatrix} \quad \ldots\ldots \quad (2)$$

Where k_u and k_v are the pixel numbers per unit of distance. $\{\mu_0, \nu_0\}$ are the origin coordinates of the camera frame in pixels, generally defined as $\{0,0\}$. φ is the angle between axes μ and ν in the image frame. F is the focal distance of the camera. These intrinsic camera parameters are acquired and calibrated in advance. Without loss of generality, we assume that these intrinsic parameters have been determined as follows: $\varphi = \pi/2$, $\mu_0 = \nu_0 = 0$, i.e., the principal point coincides with the origin of the image coordinate, and $k_u = k_v = 1$. The matrix K value is acquired as follows:

$$K = \begin{bmatrix} F & 0 & 0 \\ 0 & F & 0 \\ 0 & 0 & 1 \end{bmatrix} \quad \ldots\ldots\ldots\ldots \quad (3)$$

So we get:

$$\begin{bmatrix} \mu \\ \nu \end{bmatrix} = F \begin{bmatrix} \dfrac{x_c}{z_c} \\ \dfrac{y_c}{z_c} \end{bmatrix} \quad \ldots\ldots\ldots\ldots \quad (4)$$

2.2. Dynamics Model

A well-known equation [16], [17] describes the relationship between camera coordinate $\{O_c, x_c, y_c, z_c\}$ and system input $u = [\ \upsilon \quad \omega\ ]^T$.

$$\begin{bmatrix} \dot{x}_c \\ \dot{y}_c \\ \dot{z}_c \end{bmatrix} = -\upsilon - \omega \times \begin{bmatrix} x_c \\ y_c \\ z_c \end{bmatrix} \quad \ldots\ldots\ldots \quad (5)$$

In which υ is linear velocity and ω is the angular velocity of the robot. In the DDRs system, however, there is only two degrees of freedom (DOFs) for control i.e., υ_z, ω_y, so the dynamics model of the DDRs system is expressed as follows:

$$\begin{bmatrix} \dot{x}_c \\ \dot{y}_c \\ \dot{z}_c \end{bmatrix} = \begin{bmatrix} 0 & z_c \\ 0 & 0 \\ -1 & -x_c \end{bmatrix} \begin{bmatrix} \upsilon_z \\ \omega_y \end{bmatrix} \quad \ldots\ldots \quad (6)$$

3. Switched Extended KF

3.1. Extended KF

To estimate coordinate values of feature points in the camera frame, the state vector of robot system is defined as follows:

$$x = [\ x_c \quad y_c \quad z_c\ ]^T \quad \ldots\ldots\ldots\ldots \quad (7)$$

The discrete dynamic model is describe as follows:

$$x_k = f(x_{k-1}, u_{k-1}) + \gamma_{k-1} \quad \ldots\ldots\ldots \quad (8)$$

γ_k is the input disturbance noise vector assumed to be a zero-mean Gaussian distribution with covariance Q_k, i.e.,

$$E[\gamma_i] = q_i,\ E\left[(\gamma_i - q_i)(\gamma_i - q_j)^T\right] = Q_i \quad \ldots \quad (9)$$

Where q_i true mean and Q_i are and true moments concerning the mean of input noise sequences. It is reasonable to assume that the relative gradient of a state vector is considered constant during every small sample period only if the sample period is sufficiently small.

$$f(x_{k-1}, u_{k-1}) = x_{k-1} + T\dot{x}_{k-1} \quad \ldots\ldots\ldots \quad (10)$$

T is the sample period and k is the sample step. Using Eq. (6), the state model equation is expressed as follows:

$$f(x_{k-1}, u_{k-1}) = \begin{bmatrix} x_{c_{k-1}} + T\omega_{y_{k-1}} z_{c_{k-1}} \\ y_{c_{k-1}} \\ z_{c_{k-1}} - T\left(\upsilon_{z_{k-1}} + \omega_{y_{k-1}} x_{c_{k-1}}\right) \end{bmatrix} \quad (11)$$

After using the projection model given by Eqs. (1) and (2), it is reasonable to define the output model in terms of state vector x_k as follows:

$$y_k = g(x_k) + v_k \quad \ldots\ldots\ldots\ldots\ldots (12)$$

With measurement for feature point p_i

$$y_k = [\ \mu \quad v\ ]^T \quad \ldots\ldots\ldots\ldots\ldots (13)$$

And

$$g(x_k) = F \begin{bmatrix} \frac{x_{c_{k-1}}}{z_{c_{k-1}}} & \frac{y_{c_{k-1}}}{z_{c_{k-1}}} \end{bmatrix}^T \quad \ldots\ldots\ldots (14)$$

In which x_c, y_c, and z_c are state variables given by Eq. (7). v_k is image parameter measurement noise. Similar to γ_i, v_k is assumed to a zero-mean Gaussian distribution with covariance R_k, i.e.,

$$E[v_i] = r_i, E\left[(v_i - r_i)(v_i - r_i)^T\right] = R_i \quad \ldots\ldots (15)$$

Where r_i are true mean and R_i are and true moments concerning the mean of measurement noise sequences. From Eqs. (8) and (12), we know that the DDRs system is nonlinear. To solve this nonlinearity, we use a linearization process at each step to approximate the DDRs system an approach called KF extension (EKF).

As defined in Eq. (7), x_k is the state vector, so we defined $\hat{x}_{k,k-1}$as an a priori state estimate at step k by using information at the end of step $k-1$. $\hat{x}_{k,k}$ denotes an a posteriori estimate at step k by using measurement y_k. We define a priori and a posteriori estimate errors, and their corresponding covariances as follows:

$$e_k = x_k - \hat{x}_{k,k}, \ P_{k,k} = E\left[e_k e_k^T\right] \quad \ldots\ldots (16)$$

$$e_{k,k-1} = x_k - \hat{x}_{k,k-1}, P_{k,k-1} = E\left[e_k e_{k-1}^T\right] \quad \ldots (17)$$

EKF mainly consist of three parts i.e., linearization, prediction and estimation. EKF estimation process is described as follows:

Linearization:

$$\hat{A}_k = \frac{\partial f(x_k, u_k)}{\partial x_k}|_{x=\hat{x}_{k,k}}, \hat{C}_k = \frac{\partial g(x_k)}{\partial x_k}|_{x=\hat{x}_{k,k-1}} \quad \ldots (18)$$

Prediction:

$$\hat{x}_{k,k-1} = \hat{A}_{k-1}\hat{x}_{k-1,k-1}$$
$$P_{k,k-1} = \hat{A}_{k-1}P_{k-1,k-1}\hat{A}_{k-1}^T + Q_{k-1} \quad \ldots\ldots (19)$$

Update Kalman gain:

$$K_k = P_{k,k-1}\hat{C}_k^T\left(R_k + \hat{C}_k P_{k,k-1}\hat{C}_k^T\right)^{-1} \quad \ldots\ldots (20)$$

Update the estimation:

$$\hat{x}_{k,k} = \hat{x}_{k,k-1} + K_k(y_k - y(\hat{x}_{k,k-1}))$$
$$P_{k,k} = P_{k,k-1} - K_k\hat{C}_k P_{k,k-1} \quad \ldots\ldots\ldots (21)$$

Here, K_k are Kalman gains at step k. From [11], input disturbance noise and measurement noise covariances Q_k and R_k are considered constants during the servoing process. Both Q_k and R_k are acquired through experiments [18]. This is done to estimate the state of only one feature point p_i. Similar to this approach, we acquire states of multipoint states.

3.2. Improvement

Without improvement, the EKF technique can only enhance the precision of state measurement. To eliminate the FOV constraint, we must make the best use of the prediction function of EKF, so we define state flags I_i to indicate whether feature point P_i is captured by the camera:

$$I_{i_k} = \begin{cases} 0; & \text{if} \quad P_i \quad \text{is not captured at step} \ \ k \\ 1; & \text{if} \quad P_i \quad \text{is captured at step} \ \ k \end{cases} \quad (22)$$

When P_i is captured, we use the EKF in the usual way. If P_i is not captured, we use the prediction function of EKF to predict state vector x_k of P_i. So new Kalman filter gain $\overline{K}_k$ is defined as follows:

$$\overline{K}_k = I_{i_k}P_{k,k-1}\hat{C}_k^T\left(R_k + \hat{C}_k P_{k,k-1}\hat{C}_k^T\right)^{-1} \quad \ldots (23)$$

Updating estimation:

$$\hat{x}_{k,k} = \hat{x}_{k,k-1} + \overline{K}_k\left(y_k - y(\hat{x}_{k,k-1})\right) \quad \ldots\ldots (24)$$

$$P_{k,k} = P_{k,k-1} - \overline{K}_k\hat{C}_k P_{k,k-1} \quad \ldots\ldots\ldots (25)$$

It is clear that when the feature point is not captured, $\hat{x}_{k,k}$ equals prediction value $\hat{x}_{k,k-1}$, and $P_{k,k}$ equals $P_{k,k-1}$. Results of simulation and experiments in the next section verify the effectiveness of our method.

4. Simulation and Experiments

4.1. Simulation

Simulation results are provided to validate the proposed approach. The landmark consists of 10 feature points not located on the same vertical plane. The initial position and the desired position are respectively chosen as follows:

$$x_0 = 1; \ y_0 = 2; \ \theta_0 = \frac{\pi}{2}$$
$$x_d = 0; \ y_d = 0; \ \theta_d = \frac{\pi}{2} \quad \ldots\ldots\ldots (26)$$

From [18] noise covariance matrices were approximated using offline tuning with $q = 10^{-5}$:

$$Q = diag\,[0,\ q,\ 0,\ q,\ 0,\ q,\ 0,\ q,\ 0,\ q] \quad \ldots\ldots (27)$$

And $r = 0.01$ for:

$$R = diag\,[r,\ r,\ r,\ r,\ r,\ r,\ r,\ r,\ r,\ r] \quad \ldots\ldots\ldots (28)$$

The camera intrinsic matrix is chosen as the parameters of a real calibrated camera. Simulated images are captured with 10 frames/s with a resolution of 720×720 pixels.

Figure 2 shows the motion trajectory of the mobile robot in a 3-D scene. The visual servoing strategy we used is epipolar-based visual servoing proposed by Gian Luca Mariottini [19].

Figure 3 shows the corresponding 2D image trajectory of feature points in the pixel coordinate, where blue triangles denote the position of image features in the initial image, and red rounds denote those in the desired image.

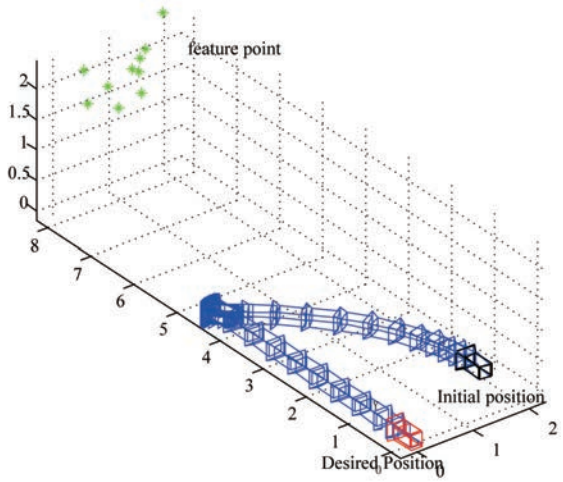

Fig. 2. 3-D trajectory of the mobile robot.

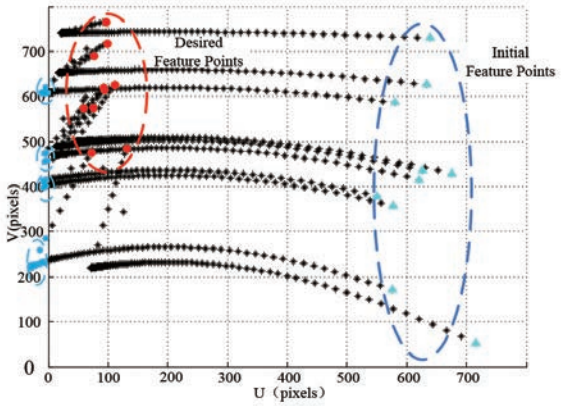

Fig. 3. Image trajectories of feature points.

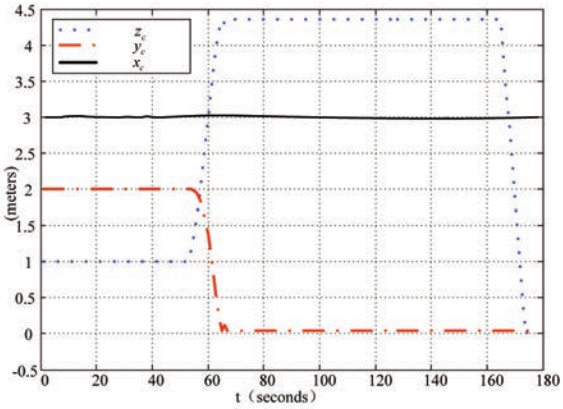

Fig. 4. Estimations of state vector x.

Even if feature points escape beyond the FOV, the robot still accomplishes the servoing task.

Figure 4 show estimation of the state vector generated in simulation. The robot obtains the state vector during all the servoing processes.

Table 1 indicates the computation cost for different temporal-filtering based algorithms used for state vector estimation. The Matlab 5 tic toc option has been used for flops calculation, and computational time was acquired using a 2.20 GHz PC with 4.00-GB RAM. Compared to Particle Filter (PF), SEKF takes less time for computation. Although EKF takes least time in these three methods, EKF can not accomplish the servoing task if feature points leave beyond the field of view. Taken together, SEKF accomplishes the servoing task effectively.

Table 1. Computational cost of state vector estimation.

Method	Flops	CPU time
PF	3036	0.0017
EKF	2997	0.0012
SEKF	3012	0.0015

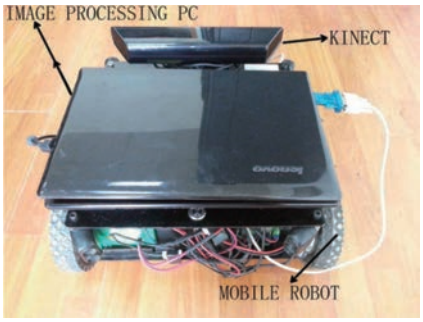

Fig. 5. Mobile robot used for the experiments.

4.2. Experiments

As shown in **Fig. 5**, the mobile robot in our system consists of the following components: a differential drive mobile robot with an Samsung ARM S3C 2410, a kinect camera that captures 30 frames per second with an 8-bit RGB image at 640 × 480 resolution, and a Intel core i5 in the PC operating under the Ubuntu 10.04 operating system, a Linux kernel based operating system. Internal mobile robot controller Samsung ARM S3C 2410 hosts the control algorithm written in Linux-C/C++. The first PC is used for image processing. The kinect camera is produced by Microsoft.

Results of experiments are illustrated in **Fig. 6**, where **(a)** is the initial robot configuration and the picture captured by the camera. The rest is the picture during the servoing process. Feature points are outside the camera FOV in **(d)** and **(e)**, the virtual task is accomplished.

To illustrate the advantage of SEKF, we also tested the PF and EKF performance and records total time for visual servoing as shown in **Table 2**.

As shown in **Table 2**, PF take more time for visual servoing. EKF cannot accomplish the servoing task. SEKF shows better performance than PF and EKF.

4.3. Extension

The proposed temporal-filtering method is applied directly in other differential visual servoing control such as the homography-based Visual Servo proposed by Yongchun Fang [20] because they share the same mathematical model.

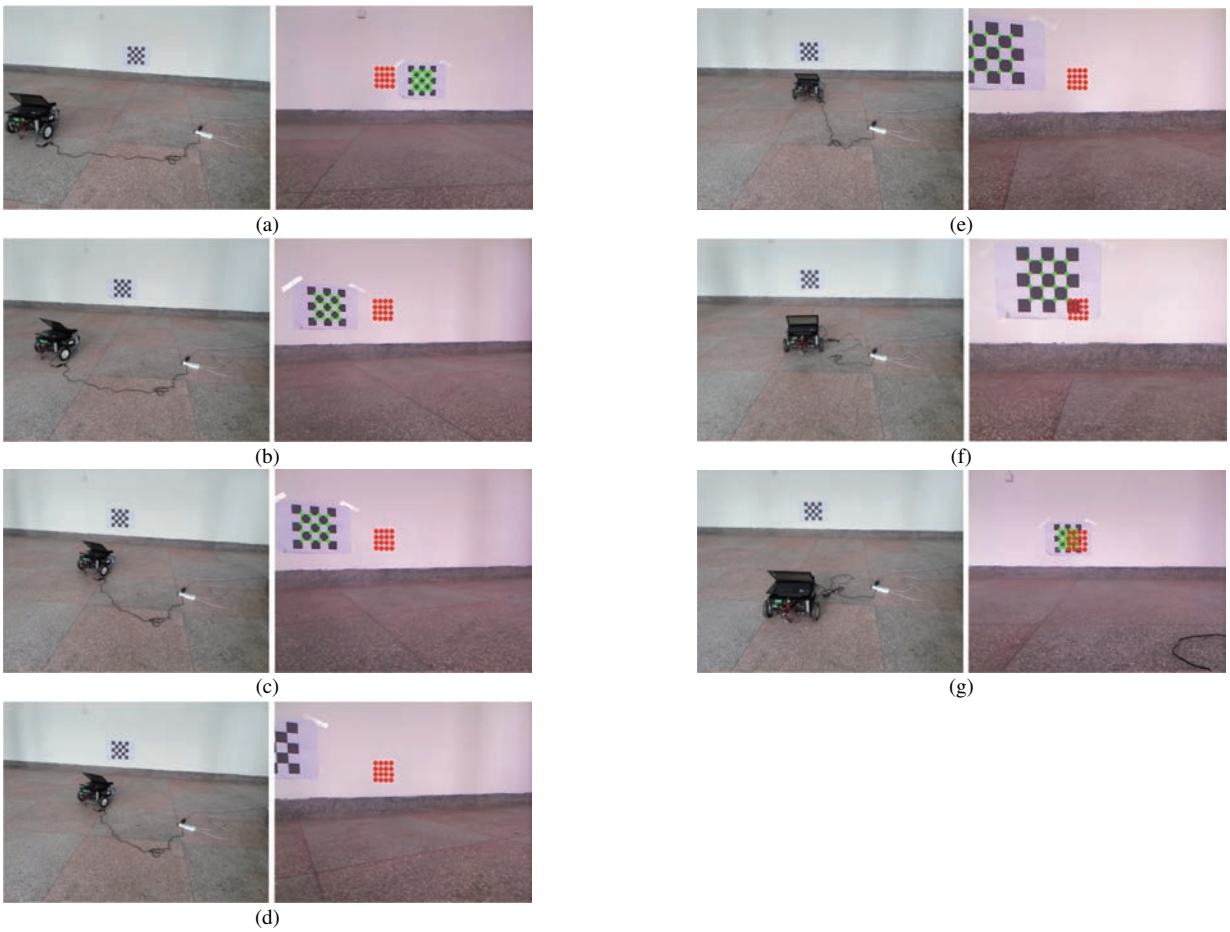

Fig. 6. Visual servoing process and real-time camera picture.

Table 2. Total servoing task time.

Method	Total time
PF	10 min 26 sec
EKF	Not accomplished
SEKF	7 min 51 sec

For the 6 DOF robot systems, we must first build the mathematical model, then use the idea proposed in this paper to accomplish the servoing task.

5. Conclusions

We have proposed a switched Kalman filter using the prediction function to solve the FOV problem. When feature points are captured, we use EKF in the usual way. When feature points go beyond the camera FOV, we use the EKF prediction function to predict the state vector. Results of Simulation and experiments confirmed that the mobile robot accomplishes the servoing task with FOV constaints.

Acknowledgements

The authors would like to acknowledge that this work was partially supported by the National Natural Science Foundation of China (Grant Nos. 61379111, 61202342, 61402538, and 61403424) and Research Fund for the Doctoral Program of Higher Education of China (Grant No. 20110162110042).

References:

[1] A. C. Sanderson and L. E. Weiss, "Image–based visual servo control using relational graph error signals," Proc. IEEE Int. Conf. On Robotics and Automation, pp. 1074-1077, 1980.
[2] S. Hutchinson, G. Hager, and P. I. Corke, "A tutorial on visual servo control," IEEE Trans. Robot. Autom., Vol.12, No.5, pp. 651-670, Oct. 1996.
[3] F. Chaumette and S. Hutchinson, "Visual servo control Part I: Basic approaches," IEEE Robot. Autom. Mag., Vol.13, No.4, pp. 82-90, Dec. 2006.
[4] F. Chaumette and S. Hutchinson, "Visual servo control Part II: Advanced approaches," IEEE Robot. Autom. Mag., Vol.14, No.1, pp. 109-118, Mar. 2007.
[5] Y. Mezouar and F. Chaumette, "Path planning for robust image-based control," IEEE Trans. Robot. Autom., Vol.18, No.4, pp. 534-549, Aug. 2002.
[6] G. Chesi and Y. S. Hung, "Global path-planning for constrained andoptimal visual servoing," IEEE Trans. Robot., Vol.23, No.5, pp. 1050-1060, Oct. 2007.
[7] X. Zhang, Y. Fang, and X. Liu, "Motion-Estimation - Based Visual Servoing of Nonholonomic Mobile Robots" IEEE Trans. 2011 on Robotics, Vol.27, No.6, pp. 1167-1175, Dec. 2011.
[8] G. López-Nicolás and S. Bhattacharya, "Switched homography-based visual control of differential drive vehicle swith field-of-viewconstraints,"Proc. IEEE Int. Conf. Robot. Autom., pp. 4238-4244, 2007.
[9] Y. Fang, X. Liu, and X. Zhang, "Adaptive Active Visual Servoing of Nonholonomic Mobile Robots" IEEE Trans. on Industrial Electronics, Vol.59, No.1, pp. 486-479, Jun. 2012.
[10] R. M. Haralick, H. Joo, C. Lee, X. Zhang, V. Vaidya, and M. Kim, "Pose estimation from corresponding point data," IEEE Trans. Syst., Man, Cybern., Vol.19, No.6, pp. 1426-1446, Nov./Dec. 1989.

[11] W. J. Wilson, C. W. Hulls, and G. S. Bell, "Relative end-effector controlusing Cartesian position based visual servoing," IEEE Trans. on Robot. Autom., Vol.12, No.5, pp. 684-696, Oct. 1996.
[12] F. Janabi-Sharifi, "Visual servoing: Theory and applications," in Opto-Mechatronic Systems Handbook, H. Cho, Ed. Boca Raton, FL: CRC, pp. 15-1–15-24, 2002.
[13] W. J. Wilson, C. W. Hulls, and F. Janabi-Sharifi, "Robust image processing and position-based visual servoing," Robust Vision for Vision-Based Control of Motion, M. Vincze and G. D. Hager (Eds.), New York, IEEE Press, pp. 163-201, 2000.
[14] R. Hartley and A. Zisserman, "Multiple View Geometry in Computer Vision," Cambridge, U.K., Cambridge Univ. Press, 2000.
[15] Y. Ma, S. Soatto, J. Kŏsecká, and S. S. Sastry, "An Invitation to 3-D Vi-sion: From Images to Geometric Models," New York, Springer, 2003.
[16] K. Deguchi, "Optimal motion control for image-based servoing by de-coupling translation and rotation," Proc. Int. Conf. Intelligent Robotsand Systems, pp. 705-711, Oct. 1998.
[17] R. Hartley and A. Zisserman, "Multiple View Geometry in Computer Vision," Cambridge, U.K., Cambridge Univ. Press, 2000.
[18] J. Wang and W. J. Wilson,"3D relative position and orientation estimation using Kalman filtering for robot control," IEEE Int. Conf. Robot. Autom., Nice, France, pp. 2638-2645, 1992.
[19] G. L. Mariottini, G. Oriolo, and D. Prattichizzo, "Image-Based Visual Servoing for Nonholonomic Mobile Robots Using Epipolar Geometry," IEEE Trans. on Robotics, Vol.23, No.1, pp. 87-100, 2007.
[20] Y. Fang, W. E. Dixon, D. M. Dawson, and P. Chawda, "Homographybased visual servo regulation of mobile robots," IEEE Trans. Syst., Man, Cybern. B, Cybern., Vol.35, No.5, pp. 1041-1050, Oct. 2005.

Name:
Yuan Fang

Affiliation:
School of Information Science and Engineering, Central South University

Address:
Changsha, Hunan 410075, China

Brief Biographical History:
2009-2013 Bachelor of Engineering, School of Information Science and Engineering, Central South University
2013- M.D. Student, School of Information Science and Engineering, Central South University

Main Works:
• Robot control and visual servoing.

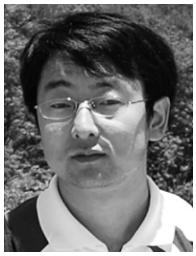

Name:
Zhang Xiaoyong

Affiliation:
Professor, School of Information Science and Engineering, Central South University

Address:
Changsha, Hunan 410075, China

Brief Biographical History:
2005/2009 Received the M.S. and D.S. degrees in Computer Application technology from Central South University

Main Works:
• "Confidence-Level-Based New Adaptive Particle Filter for Nonlinear Object Tracking," Int. J. of Advanced Robotic Systems, Vol.9, pp. 1-11, Oct. 2012.

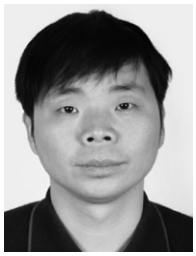

Name:
Huang Zhiwu

Affiliation:
Professor, School of Information Science and Engineering, Central South University

Address:
Changsha, Hunan 410075, China

Brief Biographical History:
1987 Received the B.S. degree in Industrial Automation from Xiangtan University
1989 Received the M.S. degree in Industrial Automation from Department of Automatic Control, University of Science and Technology Beijing
2006 Received the Ph.D. degree in Control Theory and Control Engineering from Central South University

Main Works:
• Cooperative control and Fault diagnostic technique.

Name:
Wentao Yu

Affiliation:
School of Information Science and Engineering, Central South University

Address:
Changsha, Hunan 410075, China

Brief Biographical History:
2010- Central South University

Main Works:
• "An Adaptive Unscented Particle Filter Using Relative Entropy for Mobile Robot Self-Localization," Mathematical Problems in Engineering, Vol.567373, pp. 1-9, Nov. 2013.
• "A Cooperative Path Planning Algorithm for Multiple Mobile Robot System under Dynamic Environment," Int. J. of Advanced Robotic Systems, Vol.11, pp. 1-11, Aug. 2014.

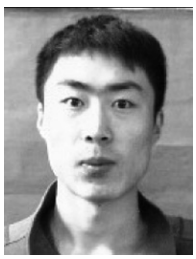

Name:
Yabo Wang

Affiliation:
chool of Information Science and Engineering, Central South University

Address:
Changsha, Hunan 410075, China

Brief Biographical History:
2009-2013 Bachelor of Engineering, School of Information Science and Engineering, Central South University
2013- M.D. Student, School of Information Science and Engineering, Central South University

Main Works:
• Robot control and path planning.